Materials and Structures (2010) 43:543–556
DOI 10.1617/s11527-009-9510-2

ORIGINAL ARTICLE

Analytical modelling of concrete cover cracking caused by corrosion of reinforcement

Leonid Chernin · Dimitri V. Val · Konstantin Y. Volokh

Received: 10 March 2008 / Accepted: 19 May 2009 / Published online: 26 May 2009

Abstract Corrosion-induced cracking of the concrete cover poses a serious problem for serviceability of reinforced concrete structures. In the paper a new analytical model for predicting cover cracking due to corrosion of reinforcing steel is presented. In the model, concrete around a corroding reinforcing bar is considered as a thick-walled cylinder subjected to uniform pressure at its inner surface, which represents expansion caused by corrosion products. The pressure leads to formation of radial cracks near the inner surface of the cylinder. In order to account for it, the cylinder is divided into two parts—a partially cracked inner cylinder and an uncracked outer one. Cracks in the inner cylinder are taken into account by gradually reducing its tangential stiffness along the radial direction. The model ensures a consistent stress-strain description within both inner and outer cylinders and complete continuity of stresses and strains on the boundary between the cylinders that distinguish it from previously published analytical models. The model is calibrated using available experimental data and then employed to estimate the amount of corrosion products penetrated into concrete pores before full cracking of the concrete cover. Estimates obtained in the paper show that this amount may be higher than has been assumed previously.

Keywords Concrete cover · Cracking · Corrosion · Reinforced concrete · Analytical model

L. Chernin · K. Y. Volokh
Department of Civil and Environmental Engineering, Technion, 32000 Haifa, Israel

D. V. Val (✉)
School of the Built Environment, Heriot-Watt University, Edinburgh EH14 4AS, UK
e-mail: D.Val@hw.ac.uk

1 Introduction

The main cause of deterioration of reinforced concrete (RC) structures is corrosion of reinforcing steel due to carbonation and/or chloride contamination of concrete (e.g., [1]). Usually, corrosion-induced concrete cover cracking, which affects the normal performance of a RC structure, appears before corrosion has any significant influence on the strength of the structure [2]. At the same time, appearance of corrosion-induced cracks on the surface of a RC structure is the main visual indicator of the corrosion presence in the structure. Thus, accurate prediction of the time to corrosion-induced cracking is necessary for estimating durability of new RC structures and management of existing RC structures.

A variety of models have been proposed to predict cracking of the concrete cover due to corrosion of reinforcing steel, which can be broadly divided into three groups: (i) empirical models (e.g., [3]),

(ii) analytical models (e.g., [4–6]), and (iii) numerical models (e.g., [7, 8]). One of the first numerical studies of corrosion-induced cracking of the concrete cover using two-dimensional finite element analysis was undertaken by Molina et al. [7]. In the study nonlinear constitutive behaviour of concrete, including cracking was described by the so-called smeared-fixed-crack model with linear softening, while the expansive nature of corrosion products was modelled using thermal analogy. A nonlinear solution was obtained using a modified Newton–Raphson algorithm. The study considered not only the initiation of cracks in the concrete cover but also the following crack propagation. Comparison of numerical results with results of the tests performed by the authors showed relatively poor agreement that was attributed to diffusion of a part of the formed corrosion products into the surrounding porous concrete [7].

Since the present article concentrates on analytical modelling, only existing analytical models are reviewed in more detail further in the article. A new analytical model proposed by the authors is then described. Like the previously proposed analytical models, the model is based on a thick-walled cylinder approach, in which the concrete surrounding a corroding reinforcing bar is considered as a thick-walled hollow cylinder with the wall thickness equal to that of the concrete cover. The corrosion-induced load, which arises due to a larger volume of the corrosion products compared to that of the consumed steel, is represented by a uniform pressure applied to the inner surface of the cylinder. The pressure leads to formation of radial cracks near the inner surface of the cylinder after which it is divided into two cylinders—a cracked inner cylinder and an uncracked outer one. Concrete in the outer cylinder is treated as an isotropic linearly elastic material. Cracks in the inner cylinder are considered as smeared and their influence is taken into account by gradually reducing the stiffness of concrete in the tangential direction of the cylinder, which is described by a power function of the radial coordinate; the stiffness in the radial direction remains unchanged. Thus, concrete in the inner cylinder is treated as an inhomogeneous orthotropic linearly elastic material, whose constitutive behaviour is modelled based on anisotropic elasticity [9]. The model ensures a consistent stress-strain description within both inner and outer cylinders and complete continuity of stresses and strains on the boundary between the cylinders that distinguish it from previously published analytical models.

The model is calibrated using available experimental data. It should be noted that results of experiments involving actual corrosion of reinforcing steel cannot be used for this purpose since corrosion products diffuse through concrete pores and microcracks so that internal pressure acting on the surrounding concrete cannot be estimated accurately. In the paper a specific set of experimental data is used, in which cracking of the concrete cover is initiated by direct application of pressure within holes made in concrete specimens [10]. It is shown that results yielded by the model are in good agreement with results of nonlinear finite element analysis. The model is then employed to estimate the amount of corrosion products diffused into concrete pores and microcracks before the concrete cover cracking. Estimates obtained in the paper show that this amount may be higher than has been assumed previously. Moreover, results presented in the paper demonstrate that a currently used approach to model the penetration of corrosion products into concrete pores and cracks based on the assumption of a finite-thickness "porous" zone around a reinforcing bar [5] leads to physically incorrect results. Explanation of why it happens is then provided and a new approach to account for the penetration of corrosion products into the surrounding concrete is proposed.

2 Critical review of existing analytical models

The first analytical model for prediction of corrosion-induced cracking of the concrete cover was proposed by Bazant [4]. In the model, concrete surrounding a corroding reinforcing bar is considered as a homogeneous linear elastic material. Expansion due to a larger volume of corrosion products compared to that of the lost steel is modelled by a uniform increase, Δd, in the diameter of the cylindrical hole around the reinforcing bar. Deformations of the corrosion products and the remaining steel are not taken into account and Δd is found from

$$\frac{\pi}{4}\left[(d+\Delta d)^2 - d^2\right] = \frac{W_{rust}}{\rho_{rust}} - \frac{W_{steel}}{\rho_{steel}} \quad (1)$$

where W_{rust} and W_{steel} are the masses of the corrosion products and the lost steel per unit length of the

reinforcing bar, respectively, and ρ_{rust} and ρ_{steel} the corrosion product and steel densities. Since $\Delta d << d$ Δd^2 can be neglected, while W_{steel} can be expressed via W_{rust} as $W_{steel} = \gamma W_{rust}$, where γ is the ratio of the molecular weight of iron to that of corrosion products, so that the following formula for Δd can be derived from Eq. 1

$$\Delta d = \frac{2W_{rust}}{\pi d}\left(\frac{1}{\rho_{rust}} - \frac{\gamma}{\rho_{steel}}\right) \quad (2)$$

To estimate W_{rust} at time t after corrosion initiation it is assumed that the rate of rust production, J_{rust}, does not change with time so that

$$W_{rust} = J_{rust}t \quad (3)$$

A relationship between the expansion Δd and the pressure, P, caused by it, is found as the average of two solutions of the classic Lamé problem—one for a hollow thick-walled cylinder under plane stress (e.g., [11])

$$\Delta d = \frac{d}{E_{c,ef}}\left[1 + v_c + \frac{d^2}{2c(c+d)}\right]P \quad (4)$$

and the other one for a circular cavity in an infinite medium (obtained an asymptotic result from Eq. 4 when $c \to \infty$)

$$\Delta d = \frac{d}{E_{c,ef}}(1 + v_c)P \quad (5)$$

where c is the thickness of the concrete cover, v_c the Poisson's ratio of concrete, $E_{c,ef} = E_c/(1 + \phi)$ the effective modulus of elasticity of concrete, E_c the modulus of elasticity of the concrete at age of 28 days, and ϕ the concrete creep coefficient. It is assumed that concrete cover cracking occurs after a long time since corrosion initiation so that $\phi = 2$ corresponding to time $t = \infty$ is adopted. The concrete cover is fully cracked when the average tensile stress in it becomes equal to the tensile strength of concrete, f_{ct}, that is equivalent to assuming perfectly plastic behaviour of the concrete before cracking. The average tensile stress is estimated as the average tangential stress in the cylinder wall so that the internal pressure causing the concrete cover cracking, P_{cr}, equals

$$P_{cr} = \frac{2cf_{ct}}{d} \quad (6)$$

Thus, if J_{rust}, ρ_{rust}, and γ are known then the time from corrosion initiation to full cracking of the concrete cover (referred further as the time to crack initiation) can be found by substituting Eqs. 2, 3 and 6 into the average of Eqs. 4 and 5.

However, comparison with experimental results showed that the Bazant's model [4] significantly underestimated the time to crack initiation [5]. In order to improve the agreement between analytical and experimental results Liu and Weyers [5] suggested modifications to the Bazant's model. First, they assumed that there was the so-called "porous" zone of finite thickness around a reinforcing bar and corrosion products accumulating around the bar did not exert any pressure on the surrounding concrete until they fully filled this zone. Note that since all concrete is porous the term "porous" zone is not a proper one in this context—it would be more correct to call this zone as the corrosion product diffusion/deposit zone; however, following Liu and Weyers [5] this term has been used in a number of publications, thus, in order to avoid confusion it is used in this paper as well. Introducing this assumption Liu and Weyers intended to account for the fact that part of corrosion products diffused into concrete pores and microcracks and, therefore, did not contribute to the pressure exerted on the concrete; this was initially suggested by Molina et al. [7] and then also observed in tests (e.g., [12]). As a result, the thickness of the porous zone, δ_0, became one of the main parameters of the model and the expansion of concrete around a corroded reinforcing bar previously estimated by Eq. 2 was expressed as

$$\Delta d = \frac{2W_{rust}}{\pi d}\left(\frac{1}{\rho_{rust}} - \frac{\gamma}{\rho_{steel}}\right) - 2\delta_0 \quad (7)$$

Second, only Eq. 4—the solution for a thick-walled cylinder (Fig. 1a), was used to establish the relationship between the expansion Δd and the corresponding pressure P (and not the average of Eqs. 4 and 5). Third, it was assumed that the rate of rust production, J_{rust}, was not constant but inversely proportional to the amount of corrosion products and, hence, decreased with time. This led to the following relationship between the time to crack initiation, t_{cr}, and the critical mass of corrosion products causing cracking, $W_{rust,cr}$

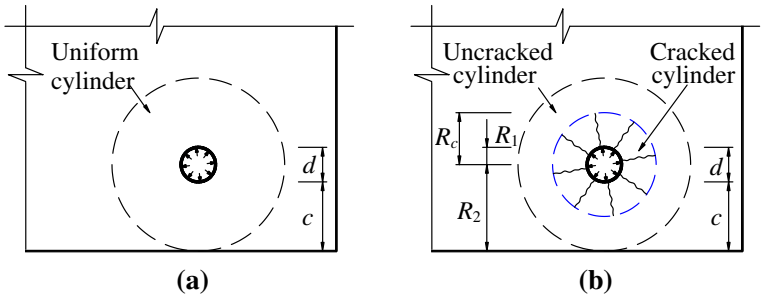

Fig. 1 Thick-walled cylinder model: **a** uniform cylinder; **b** partially cracked (composite) cylinder

$$t_{cr} = \frac{W_{rust,cr}^2}{2k_p} \tag{8}$$

where k_p had to be a time-invariant constant. $W_{rust,cr}$ was found from Eqs. 4, 6 and 7, while for k_p Liu and Weyers [5] proposed an incorrect formula, which violated Faraday's law of electrolysis (see [13] for more detailed explanation).

El Maaddawy and Soudki [14] noted that the use of the assumption about the rate of rust production decreasing with time led to underestimation of the mass of lost steel observed in accelerated corrosion tests (it is expected since in such tests the rate of rust production is constant). In their paper the rate of rust production was set constant and expressed via the corrosion current density, i_{corr}, using Faraday's law as

$$J_{rust} = \frac{M\pi d}{zF\ \gamma} i_{corr} \tag{9}$$

where M the molar mass of iron (55.85 g/mol), z the valence of the reaction (2 for $Fe \rightarrow Fe^{2+}+2e^{-}$), F Faraday's constant (96458 C/mol), and i_{corr} the corrosion current density. Thus, t_{cr} was estimated as

$$t_{cr} = \frac{W_{rust,cr}}{J_{rust}} \tag{10}$$

where $W_{rust,cr}$ was found like in [5] from Eqs. 4, 6 and 7.

A limitation of the thick-walled uniform cylinder model described above is its inability to account for non-linear behaviour of concrete, which takes place when radial cracks start to form near the inner surface of the cylinder. This is demonstrated by Fig. 2, which shows relationships between the internal pressure and the radial displacements on the inner surface yielded by the model and by non-linear finite element (FE) analysis with ABAQUS [15]; description of the FE

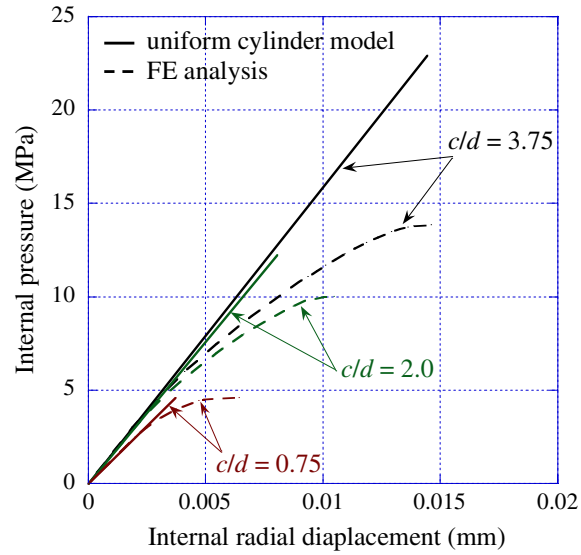

Fig. 2 Internal pressure versus internal radial displacements in the thick-walled concrete cylinder

model employed in ABAQUS can be found in [16]. The analyses were carried out for $d = 16$ mm, $f_{ct} = 3$ MPa, $E_{c,ef} = 15{,}600$ MPa, and $\nu_c = 0.2$. As expected, differences between results of the thick-walled cylinder model and the non-linear FE analysis increase with an increase in the c/d ratio (see Fig. 2).

This limitation can be overcome by partition of the cylinder into two parts: a cracked inner cylinder and an uncracked outer one (Fig. 1b). The idea was originally proposed by Tepfers [17] to model cover cracking due to bond stresses developing between a deformed reinforcing bar and the surrounding concrete. In the Tepfers solution resistance of concrete in the inner cylinder in the tangential direction normal to cracks (i.e., tension softening) was completely neglected so that the cylinder transferred only radial stresses. A number of researchers have tried to improve the Tepfers solution by taking into account

tension softening; in this review only the works directly related to modelling cover cracking due to corrosion will be mentioned. Wang and Liu [18] treated cracks in the inner cylinder as smeared (the approach which was adopted in all the models considered further in the review) and described tension softening by a bi-linear stress-strain relationship from CEB-FIP Model Code 1990 [19]. However, in order to calculate the tangential stresses in the inner cylinder they used the displacement field found from a linear elastic solution for a thick-walled uniform cylinder (as was originally proposed in [20]) that was clearly inconsistent.

Another approach was used by Bhargava et al. [21], who suggested to consider concrete in the inner cracked cylinder as an isotropic linearly elastic material with a reduced modulus of elasticity compared to that of the outer cylinder. The reduced modulus of elasticity was defined as the secant slope of the branches of the bi-linear tension softening relationship from [19]. The time to crack initiation was found from solution of a thick-walled composite cylinder made from two isotropic linearly elastic materials with different moduli of elasticity, which was subject to internal pressure. Obviously, full compatibility of both stresses and strains, which exists on the boundary between the inner cracked and the outer uncracked parts of a concrete cylinder, cannot be achieved in the model on the boundary between the two materials. In [21] only stress compatibility was ensured. Another shortcoming of the model proposed by Bhargava et al. [21] is treating cracked concrete in the inner cylinder as an isotropic material, while in reality stiffness of the concrete in the radial direction parallel to cracks is significantly higher than that in the radial direction normal to cracks (i.e., the modulus of elasticity in the radial direction was unjustly reduced).

The anisotropy of cracked concrete was taken into account by Li et al. [6], who modelled concrete in the inner cracked cylinder as an orthotropic material with the modulus of elasticity reduced only in the tangential direction normal to cracks (the modulus of elasticity in the radial direction remained unchanged and was equal to that in the outer uncracked cylinder). Although it was noted in the paper [6] that the tangential stiffness of the inner cylinder had to be a function of the radial coordinate, it was represented by a single value estimated on the basis of the average tangential strain. Thus, compatibility of both stresses and strains on the boundary between the two cylinders was not provided as well. This problem was resolved by Pantazopoulou and Papoulia [22], who took into account that the tangential stiffness of concrete in the inner cylinder changed gradually depending on the radial coordinate and the corresponding tangential strain. However, they were not able to find an analytical solution and solved the problem numerically by a finite-difference method.

It is also important to note that following Bazant [4] all the above mentioned models have used plane stress solutions. However, it is only correct for an internally pressurised hollow cylinder with free ends, while the concrete cylinder around a reinforcing bar is actually within the bulk concrete of a RC element, which prevents free deformation in the direction of the cylinder axis. Under such conditions, the use of a plane strain formulation is more correct.

3 Model description

Like the models reviewed above, the proposed model treats concrete around a corroding reinforcing bar as a thick-walled cylinder with the wall thickness equal to that of the concrete cover. In order to account for non-linear behaviour of concrete after partial cracking the cylinder is divided into two parts—an inner cylinder with cracks in the radial direction and an outer uncracked one (see Fig. 1b). Cracks in the inner cylinder are considered as smeared and the cylinder is subjected either to uniform pressure or imposed radial displacements at its inner surface. This means that the problem is axisymmetric so that the only displacement component is the radial displacement, u, which is a function of the radial coordinate, r, i.e., $u = u(r)$. If body forces are zero, the equilibrium equation for both inner and outer cylinders can then be written as

$$\frac{d\sigma_r}{dr} + \frac{\sigma_r - \sigma_\theta}{r} = 0 \tag{11}$$

where σ_r and σ_θ are the radial and tangential stresses, respectively. Strain-displacements relationships are

$$\varepsilon_r = \frac{du}{dr}; \quad \varepsilon_\theta = \frac{u}{r} \tag{12}$$

where ε_r and ε_θ are the radial and tangential strains, respectively.

3.1 Inner cylinder

The inner cylinder (i.e., the cracked part of the composite thick-walled cylinder) extends from $r = R_1$ to $r = R_c$ (see Fig. 1b). There is strong anisotropy in the behaviour of concrete in the cylinder due to radial cracks. Therefore, if in an analytical model the concrete is modelled as a linearly elastic material (which is a typical approach for thick-walled cylinder models) it is essential to take the anisotropy into account. In order to demonstrate the effect of the anisotropy, residual stiffness of concrete in both radial and tangential directions is estimated in a partially cracked thick-walled cylinder ($d = 16$ mm, $c = 50$ mm, $E_{c,ef} = 15\ 600$ MPa, $f_{ct} = 3$ MPa) loaded by internal pressure $P = 10.5$ MPa. For this purpose, non-linear FE analysis of the cylinder is carried out using the model described in [16]. Based on results of the analysis average strains and stresses over the circumferences located between R_1 and R_2 (which are the internal and external radii of the thick-walled cylinder, respectively, see Fig. 1b) are calculated in both radial ($\varepsilon_{r,av}$ and $\sigma_{r,av}$) and tangential ($\varepsilon_{\theta,av}$ and $\sigma_{\theta,av}$) directions. The residual stiffnesses in the radial and the tangential directions (denoted as $E_{r,sec}$ and $E_{\theta,sec}$, respectively) are estimated as secant values

$$E_{r(\theta),\mathrm{sec}} = \frac{(1-\nu_c)^2}{\varepsilon_{r(\theta),av}}\left(\sigma_{r(\theta),av} - \frac{\nu_c}{1-\nu_c}\sigma_{\theta(r),av}\right) \qquad (13)$$

Since Eq. 13 does not take into account that in the cracked part the Poisson's ratio, ν_c, has different values in the radial and tangential direction, values yielded by it should be considered only as rough estimates of the secant stiffness, which are presented here only to illustrate anisotropy of the cracked concrete. The calculated values of $E_{r,sec}$ and $E_{\theta,sec}$ normalised to $E_{c,ef}$ are shown in Fig. 3 versus the normalised radial coordinate, (r/R_2). As can be seen, the stiffness of concrete in the radial direction remains practically unchanged, while in the tangential direction it decreases significantly and can be described by a smooth function of the radial coordinate.

Thus, concrete in the inner cylinder is modelled as an inhomogeneous orthotropic linearly elastic material with the modulus of elasticity in the tangential direction, E_θ, being a power function of the radial coordinate

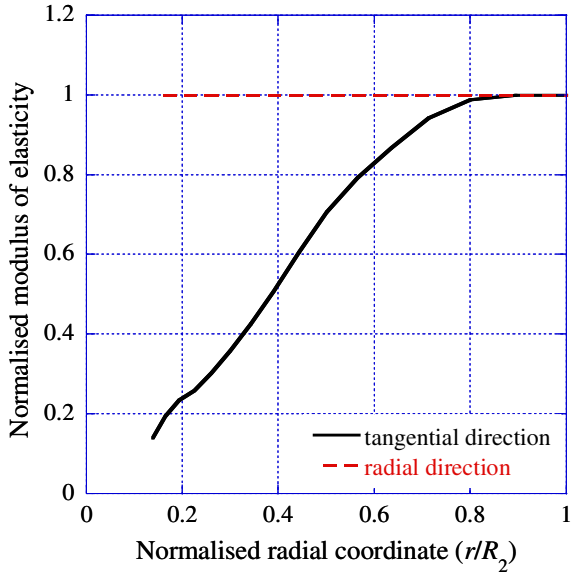

Fig. 3 Residual stiffness of partially cracked thick-walled concrete cylinder (FE analysis)

$$E_\theta(r) = E_{c,ef} f(r) = E_{c,ef}\left(\frac{r}{R_c}\right)^n \qquad (14)$$

where R_c is the radius of the inner cylinder (see Fig. 1b) and n a non-negative real number. The moduli of elasticity in the radial, E_r, and the cylinder axis, E_z, directions are constant and equal to the modulus of elasticity of uncracked concrete, i.e., $E_r = E_z = E_{c,ef}$. Generalised Hook's law in this case of cylindrical anisotropy can be expressed as [9]

$$\begin{aligned}
\varepsilon_r &= \frac{1}{E_r}\sigma_r - \frac{\nu_{\theta r}}{E_\theta}\sigma_\theta - \frac{\nu_{zr}}{E_z}\sigma_z \\
\varepsilon_\theta &= -\frac{\nu_{r\theta}}{E_r}\sigma_r + \frac{1}{E_\theta}\sigma_\theta - \frac{\nu_{z\theta}}{E_z}\sigma_z \\
\varepsilon_z &= -\frac{\nu_{rz}}{E_r}\sigma_r - \frac{\nu_{\theta z}}{E_\theta}\sigma_\theta + \frac{1}{E_z}\sigma_z
\end{aligned} \qquad (15)$$

where ε_z and σ_z are strains and stresses in the cylinder axis direction, and ν's denote the Poisson's ratios. Taking into account the symmetry requirements [9]

$$E_r\nu_{\theta r} = E_\theta\nu_{r\theta}; \quad E_z\nu_{\theta z} = E_\theta\nu_{z\theta}; \quad E_z\nu_{rz} = E_r\nu_{zr} \qquad (16)$$

it can be shown that

$$v_{r\theta} = v_{z\theta} = v_{zr} = v_{rz} = v_c; \quad v_{\theta r} = v_{\theta z} = v_c f(r) \tag{17}$$

For the plane strain formulation considered herein $\varepsilon_z = 0$ that leads to

$$\sigma_z = v_c(\sigma_r + \sigma_\theta) \tag{18}$$

From Eqs. 15, 17 and 18 the radial, $\sigma_r^{(i)}$, and the tangential, $\sigma_\theta^{(i)}$, stresses in the inner cylinder can be expressed as

$$\sigma_r^{(i)} = \frac{E_{c,ef}}{1 - v_c - 2v_c^2 f(r)}\left[\frac{1 - v_c^2 f(r)}{1 + v_c}\frac{du^{(i)}}{dr} + v_c f(r)\frac{u^{(i)}}{r}\right] \tag{19}$$

$$\sigma_\theta^{(i)} = \frac{(1 - v_c)f(r)E_{c,ef}}{1 - v_c - 2v_c^2 f(r)}\left(\frac{v_c}{1 - v_c}\frac{du^{(i)}}{dr} + \frac{u^{(i)}}{r}\right) \tag{20}$$

where $u^{(i)}$ is the radial displacement in the inner cylinder. By substituting Eqs. 19 and 20 into Eq. 11 the following differential equation is obtained

$$\begin{aligned}&\frac{1 - v_c^2 f(r)}{1 + v_c}\frac{d^2u^{(i)}}{dr^2} + \frac{1 - v_c^2\left[r\frac{df(r)}{dr} + f(r)\right]}{1 + v_c}\frac{1}{r}\frac{du^{(i)}}{dr} \\ &\quad + v_c\left[r\frac{df(r)}{dr} - \frac{1 - v_c}{v_c}f(r)\right]\frac{u^{(i)}}{r^2} \\ &\quad + HOT\left(v_c^2, v_c^3, v_c^4\right) = 0\end{aligned} \tag{21}$$

where $HOT(.,.,.)$ denotes the higher order terms, which include 2nd-, 3rd- and 4th-order terms of the Poisson's ratio

$$\begin{aligned}&HOT\left(v_c^2, v_c^3, v_c^4\right) \\ &\quad = \frac{2v_c^2}{1 - v_c - 2v_c^2 f(r)}\frac{df(r)}{dr}\left[\frac{1 - v_c^2 f(r)}{1 + v_c}\frac{du}{dr} + v_c f(r)\frac{u}{r}\right]\end{aligned} \tag{22}$$

If to neglect the higher order terms, the solution of Eq. 21 can be presented as

$$\begin{aligned}u^{(i)}(r) = {} & C_1 r^{-\lambda_1 n} F(\lambda_1, \lambda_1; 2\lambda_1; w) \\ & + C_2 r^{-\lambda_2 n} F(\lambda_2, \lambda_2; 2\lambda_2; w)\end{aligned} \tag{23}$$

where $F(.,.;.;.)$ is the hypergeometric function [23], C_1 and C_2 are the constants, and λ_1, λ_2 and w are given by the following formulas

$$\begin{aligned}&\lambda_{1(2)} = \frac{nv_c \mp \sqrt{-4 + v_c^2(n+2)^2 + 4nv_c}}{2nv_c}; \\ &w = \frac{1}{v_c^2}\left(\frac{r}{R_c}\right)^{-n}\end{aligned} \tag{24}$$

The appropriateness of neglecting the higher order terms has been examined by substituting the solution (Eq. 23) into Eq. 22 for various values of the relevant geometric and material parameters; very small values (of order of 10^{-7}) of $HOT(.,.,.)$ have been obtained.

3.2 Outer cylinder

The outer cylinder (i.e., the uncracked part of the composite cylinder) corresponds to $R_c \le r \le R_2$ (see Fig. 1b). Concrete in the cylinder is treated as an isotropic linearly elastic material with the modulus of elasticity $E_{c,ef}$ and Poisson's ratio v_c. The problem—a hollow thick-walled cylinder subjected to internal pressure, is well known in linear elasticity (e.g., [11]). In the case of the plane strain formulation the radial, $\sigma_r^{(o)}$, and the tangential, $\sigma_\theta^{(o)}$, stresses in the outer cylinder can be expressed via the radial displacement as

$$\sigma_r^{(o)} = \frac{E_{c,ef}}{(1 + v_c)(1 - 2v_c)}\left[(1 - v_c)\frac{du^{(o)}}{dr} + v_c\frac{u^{(o)}}{r}\right] \tag{25}$$

$$\sigma_\theta^{(o)} = \frac{E_{c,ef}}{(1 + v_c)(1 - 2v_c)}\left[(1 - v_c)\frac{u^{(o)}}{dr} + v_c\frac{du^{(o)}}{dr}\right] \tag{26}$$

where $u^{(o)}$ is the radial displacement in the outer cylinder. Substitution of Eqs. 25 and 26 into Eq. 11 leads to the following differential equation

$$\frac{d^2u^{(o)}}{dr^2} + \frac{1}{r}\frac{du^{(o)}}{dr} - \frac{u}{r^2} = 0 \tag{27}$$

whose solution is

$$u^{(o)}(r) = C_3\frac{r}{2} + C_4\frac{1}{r} \tag{28}$$

where C_3 and C_4 are the constants.

3.3 Boundary and compatibility conditions

To find the four constants C_1, C_2, C_3, and C_4 four boundary and compatibility (on the boundary between the two cylinders) conditions are needed. Since the outer surface (i.e., at $r = R_2$, see Fig. 1b) is traction-free the boundary condition for it is

$$\sigma_r^{(o)}(r = R_2) = 0 \quad (29)$$

There are also three compatibility conditions on the boundary between the two cylinders (i.e., at $r = R_c$, see Fig. 1b)

$$u^{(i)}(r = R_c) = u^{(o)}(r = R_c) \quad (30)$$

$$\sigma_r^{(i)}(r = R_c) = \sigma_r^{(o)}(r = R_c) \quad (31)$$

$$\sigma_\theta^{(i)}(r = R_c) = \sigma_\theta^{(o)}(r = R_c) = f_{ct} \quad (32)$$

The first and the second conditions (Eqs. 30 and 31) represent the requirement of continuity of the radial displacement and stress, respectively, while the third condition (Eq. 32) states that the tangential stress on the boundary equals the tensile strength of concrete. These three conditions ensure full compatibilty of both stresses and strains on the boundary between the two cylinders.

The radius of the inner cylinder R_c (i.e., the location of crack front) is unknown as well as boundary conditions on the inner surface (i.e., at $r = R_1$, see Fig. 1b). The aim is to determine these boundary conditions, i.e., the internal pressure and the corresponding radial displacement, at which full cracking of the cylinder wall occurs. A procedure for solving this problem and then estimating the time to crack initiation is described in the next section.

3.4 Solution procedure

In order to estimate the time to crack initiation using the proposed model the following steps need to be carried out:

- Value of R_c are incrementally increased from R_1 to R_2.
- For each value of R_c the problem is solved (i.e., the constants C_1, C_2, C_3, and C_4 are found from Eqs. 29–32), and then values of the radial displacement on the inner surface $\delta = u^{(i)}(r = R_1)$ and the internal pressure $P = -\sigma_r^{(i)}(r = R_1)$ are calculated by Eqs. 23 and 19, respectively.
- From the calculated values of P the maximum one is selected. This is the internal pressure, which causes full cracking of the cylinder wall, i.e., P_{cr}. The corresponding values of R_c and δ are denoted as $R_{c,cr}$ and δ_{cr}, respectively. Note that $l_{cr,st} = R_{c,cr} - R_1$ represents the maximum stable radial crack length since longer cracks could only be stable at internal pressures lower than P_{cr}, i.e., at P_{cr} the radial cracks should propagate through an uncracked outer part of the cylinder wall.
- To account for the penetration of part of corrosion products into concrete pores and microcracks the equivalent thickness, δ_d, representing this part of the corrosion products is introduced. Note that introducing δ_d is not equivalent to the assumption of Liu and Weyers [5] about the "porous" zone of finite thickness δ_0. The equivalent thickness, δ_d, represents all the corrosion products diffused into the surrounding concrete over the period from corrosion initiation to cover cracking and may increase constantly as a function of time, while according to the assumption about the "porous" zone δ_0 should be a constant value, i.e., after the "porous" zone has been filled no further diffusion of the corrosion products into the surrounding concrete is possible. If the corrosion rate is constant then the time to crack initiation (in years) can be estimated based on Faraday's law as

$$t_{cr} = \frac{\delta_{cr} + \delta_d}{11.6 i_{corr}(\alpha_v - 1)} \quad (33)$$

where α_v is the volumetric expansion ratio of corrosion products, i_{corr} is in $\mu A/cm^2$, and δ_{cr} and δ_d are in μm.

Thus, for the calculation of t_{cr} values of i_{corr}, α_v, δ_{cr} and δ_d need to be known. The prediction of i_{corr} is not considered herein; α_v can be set equal to three based on available experimental data [24, 25]; the evaluation of δ_d is described further in the paper; and the calculation of δ_{cr} using the proposed model is illustrated by the following example. A RC concrete member with the following properties: $d = 16$ mm, $c = 50$ mm, $E_{c,ef} = 15{,}600$ MPa and $f_{ct} = 3$ MPa, is considered. According to the model, δ_{cr} is found from the analysis of a thick-walled cylinder with $R_1 = 8$ mm and $R_2 = 58$ mm (see Fig. 1b) using the procedure described above. Figure 4 shows the relationship between the internal pressure and R_c for the cylinder; the calculations are carried out with $\nu_c = 0.2$ and $n = 2$. As can be seen, the maximum pressure 13.28 MPa is obtained for the radius of the inner cylinder of 39.9 mm (i.e., $P_{cr} = 13.28$ MPa and $R_{c,cr} = 39.9$ mm) and it corresponds to $\delta_{cr} = 17.65$ μm (not shown in Fig. 4). It should be

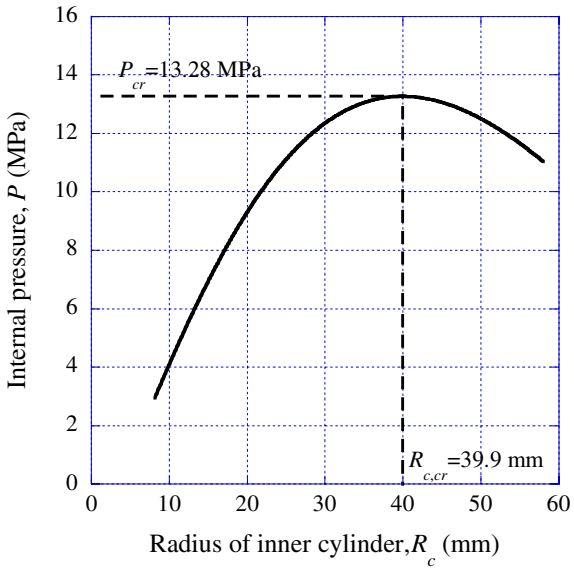

Fig. 4 Internal pressure versus the radius of the inner cracked cylinder

noted that in this example the value of n has simply been assumed for illustrative purpose, its proper evaluation is described in the next section.

4 Model calibration

In order to use the proposed model it should be calibrated, i.e., values of the two parameters—the exponent n of the power function describing the change of the modulus of elasticity with the inner cylinder (see Eq. 14) and the equivalent thickness δ_d representing the amount of corrosion products diffused into the surrounding concrete (see Eq. 33), need to be determined using available experimental data.

4.1 Estimation of the exponent n

It is desirable to estimate n independently of δ_d. Results of tests involving actual corrosion of reinforcing steel are unsuitable for this purpose since a part of forming corrosion products penetrates into concrete pores and microcracks so that expansion (i.e., imposed radial displacements) or pressure around a corroding reinforcing bar cannot be estimated accurately. In the study the model is calibrated using results of the tests carried out by Williamson and Clark [10], in which cracking of the concrete cover was caused by controlled pressure applied within cylindrical holes made in concrete specimens—150-mm cubes (the pressure was provided by a hydraulic jack through soft PVC tubes inserted into the holes). Parameters varied in the tests include the diameter of the holes (8 and 16 mm), the thickness of the concrete cover (4, 8 and 16 mm), the aggregate size (5 and 10 mm for 8-mm diameter holes, and 10 and 19 mm for 16-mm diameter holes), the hole location (at the corner or in the middle of the side of the specimens), and concrete strength (three different concrete mixes were used with the splitting tensile strength varied from 2.2 MPa to 4.1 MPa). Values of n, which provide perfect agreement between the model predictions and the test results, are shown in Fig. 5a versus the splitting tensile strength of concrete, f_{ct}. There is an increase in n with increasing f_{ct} which can be described by an exponential function, whose coefficients are found by a regression analysis (see Fig. 5a). It should be noted that the relationship between n and f_{ct} has rather poor correlation with test data ($R^2 = 0.3948$), which clearly indicates that more test data are needed to properly calibrate the model. Figure 5b shows the corresponding values of the maximum stable crack length normalised to the thickness of the concrete cover, i.e., $l_{cr,st}/c$ (%). As can be seen, the maximum stable crack length decreases as the concrete strength increases; this tendency is also indicated by the linear regression shown in Fig. 5b. This shows that the model reflects correctly the well-known phenomenon that with increasing strength concrete becomes more brittle.

The distribution of the tangential stress, σ_θ, within the inner cylinder depends strongly on n. Obviously, it is not sufficient merely to require that σ_θ equals the tensile strength of concrete, f_{ct}, on the boundary with the outer cylinder, i.e., at $r = R_c$. It is also necessary to ensure that σ_θ does not exceed f_{ct} anywhere within the inner cylinder. Moreover, it is also desirable to obtain a gradual increase of σ_θ when the radial coordinate increases from R_1 to R_c since this is expected from a physical point of view. These conditions impose a limit on the value of n. Numerical studies have showed that n should not be less than 1.5. Figure 6, which presents distributions of σ_θ at $P = P_{cr}$ for different values of n, illustrates this point. It also shows that $R_{c,cr}$ and, subsequently, the maximum stable radial crack length decrease with

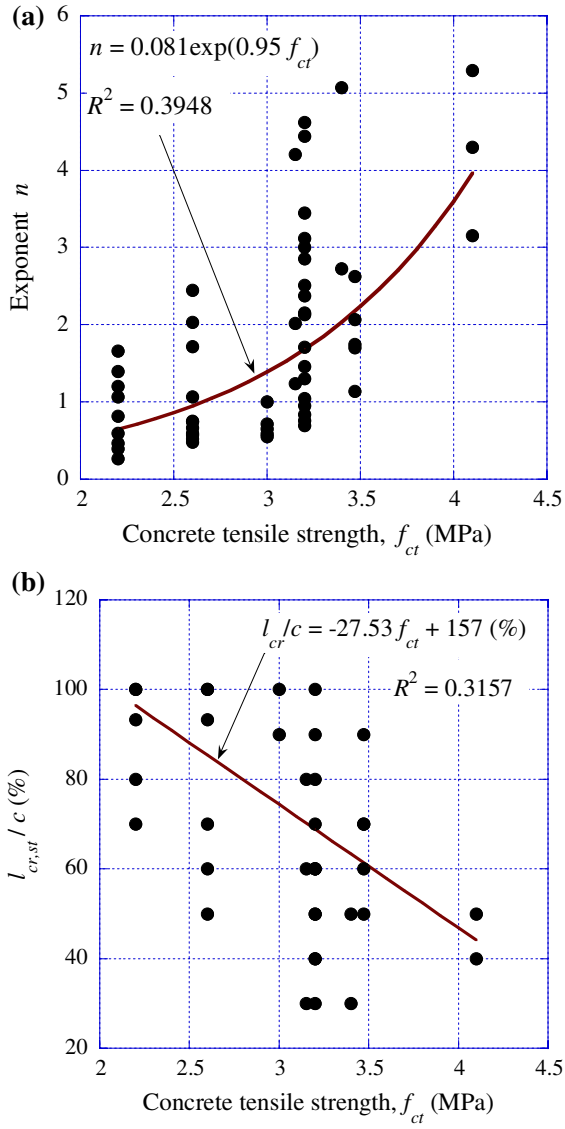

Fig. 5 Results of model calibration: **a** exponent n; **b** maximum stable crack length $l_{cr,st}$

increasing n (i.e., an increase in n leads to more brittle behaviour). The results are obtained for $d = 16$ mm, $c = 50$ mm, $E_{c,ef} = 15{,}600$ MPa, and $f_{ct} = 3$ MPa. However, the shape of the σ_θ-distribution within the inner cylinder wall does not depend on $E_{c,ef}$, f_{ct} or c/d, thus, 1.5 can be used as the lower limit of n for other values of these parameters as well. It may be noted that Fig. 6 only demonstrates that the lower limit of n should be between 1.4 and 1.5. However, the benefit of obtaining a more accurate estimate of this limit is negligible since the difference

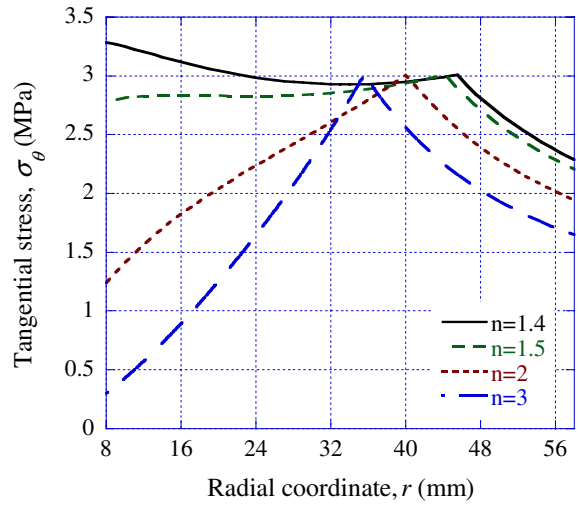

Fig. 6 Distribution of σ_θ within the cylinder wall at $P = P_{cr}$ for different values of the exponent n

in values of δ_{cr} calculated using $n = 1.4$ and $n = 1.5$ is less than 4%. Thus, based on the available data it is recommended to use the following values of n

$$n = \begin{cases} 1.5, & f_{ct} \le 3.07 \text{ MPa} \\ 0.081\exp(0.95 f_{ct}), & f_{ct} > 3.07 \text{ MPa} \end{cases} \quad (34)$$

Of course, this is a tentative recommendation since the test-based estimates of n are widely scattered (Fig. 5a) and more experimental data are needed to obtain a better estimate of n.

Comparison of values of the critical pressure yielded by the model with those obtained by FE analysis and the thick-walled uniform cylinder model is shown in Fig. 7 (the analyses have been carried out with $E_{c,ef} = 15{,}600$ MPa and $f_{ct} = 3$ MPa). As can be seen, for the c/d ratios of 0.75 and higher, the results of the proposed model (with n between 1.5 and 3) are much closer to the results of the FE analysis than those of the thick-walled uniform cylinder model.

4.2 Estimation of the amount of diffused corrosion products

The other parameter, which is needed for evaluation of the time to crack initiation, is the amount of corrosion products penetrating into concrete pores and microcracks. Currently, this amount is usually represented by the thickness of the "porous" zone, δ_0, as was initially proposed by Liu and Weyers [5].

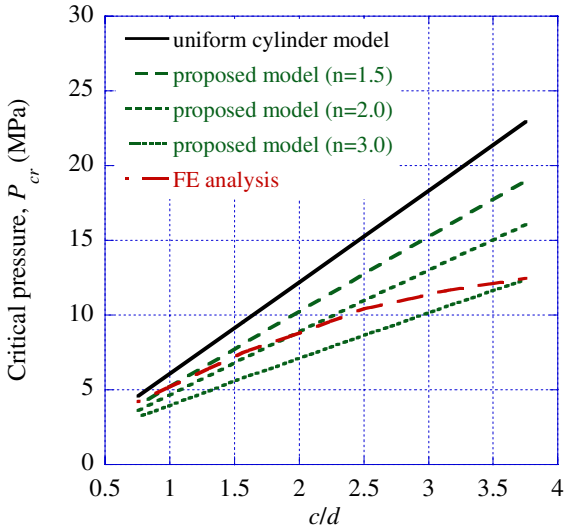

Fig. 7 Comparison of the proposed model with the thick-walled uniform cylinder model and FE analysis

They also suggested to estimate δ_0 indirectly by fitting the times to crack initiation predicted analytically to those observed in tests. Using this approach, their own experimental data, and their incorrect model (see [13]) Liu and Weyers [5] estimated that δ_0 was 12.5 μm. Petre-Lasar [26] investigated the concrete—rebar interface using a scanning electron microscope. Based on this study he proposed a formula relating δ_0 with the thickness of the concrete-rebar interface (set as 40 μm), the degree of hydration, and the water–cement ratio. According to the formula, δ_0 varies between 2 μm and 8 μm depending on the values of the degree of hydration and the water–cement ratio. El Maaddawy and Soudki [14] considered δ_0 in the range of 10–20 μm and reported a good agreement between analytical results obtained using the thick-walled uniform cylinder model and results of accelerated corrosion tests. However, in their analysis they significantly underestimated the effective modulus of elasticity of concrete by assuming that the concrete creep coefficient $\phi = 2.35$ (the value recommended by the CSA Standard A23.3-94 [27] for $t = \infty$). This assumption was incorrect since in all the accelerated corrosion tests considered in their study cracking occurred within 11 days after corrosion initiation (except of one, in which it was observed after 110 days), i.e., ϕ was close to zero and $E_{c,ef} \approx E_c$. This brief overview shows that existing estimates of δ_0 are contradictive and at least partly based on incorrect assumptions.

As noted above (see Eq. 33), in this study the amount of corrosion products diffused into the surrounding concrete is represented by the equivalent thickness δ_d. This means that no assumption about the diffusion of corrosion products is initially made, i.e., the corrosion products can diffuse either only at the beginning of the corrosion process until they fully fill the finite-thickness "porous" zone or constantly over time. The equivalent thickness is estimated indirectly using the approach proposed by Liu and Weyers [5] as the difference between test results and analytical results yielded by the proposed model

$$\delta_d = \delta_{cr,exp} - \delta_{cr} \tag{35}$$

where $\delta_{cr,exp}$ is the total expansion of corrosion products in a test at the time of cover cracking, while δ_{cr} is the radial displacement at the inner surface of the thick-walled cylinder causing its wall cracking, which is found analytically (see Sect. 3.4) with data from the test specimen. Results of a number of accelerated corrosion tests [3, 25, 28–32] are used. Since in the tests the corrosion current density is known and constant $\delta_{cr,exp}$ (in μm) can be evaluated as

$$\delta_{cr,exp} = 11.6 i_{corr} t_{cr,exp} (\alpha_v - 1) \tag{36}$$

where $t_{cr,exp}$ is the time of cover cracking in the test (in years). In the calculations the volumetric expansion ratio of corrosion products is set equal to three ($\alpha_v = 3$). It is also important to note that in the calculations the effective modulus of elasticity of concrete is evaluated using values of ϕ corresponding to $t_{cr,exp}$; the values are estimated in accordance to CEB-FIP Model Code [19].

Obtained values of δ_d versus the compressive strength of concrete, f_c, are shown in Fig. 8a. The compressive strength has been chosen for this graph since this is one of the main parameters characterising concrete properties (e.g., it is strongly correlated with the water–cement ratio, tensile strength and modulus of elasticity of concrete) and its values are provided in the description of all the tests [3, 25, 28–32] used in this study. As can be seen, in many cases the values of δ_d are much greater than 20 μm (the average value of δ_d is 28.7 μm). It can also be observed that δ_d shows a tendency to increase with an

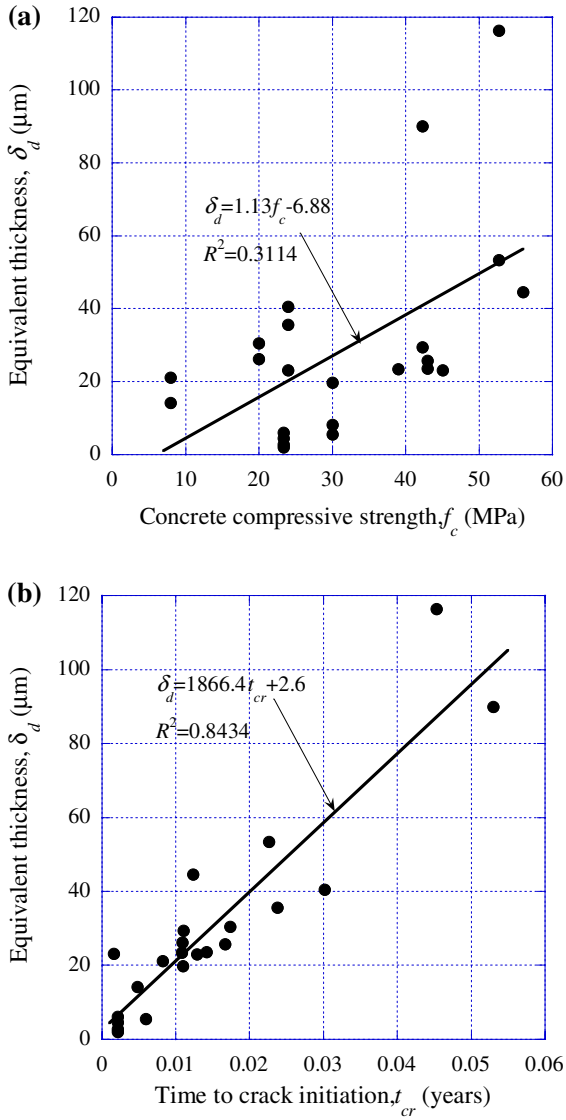

Fig. 8 Equivalent thickness representing the diffused corrosion products versus: **a** compressive strength of concrete; **b** time to crack initiation

increase in f_c. Figure 8b shows δ_d versus the time to crack initiation; there is a strong linear correlation between δ_d and t_{cr}, i.e., δ_d increases linearly with an increase in t_{cr}. If to consider these results in the context of the assumption about the finite-thickness "porous" zone (i.e., $\delta_0 = \delta_d$) there are major contradictions. First, the results indicate that the thickness of the "porous" zone increases with an increase in f_c (Fig. 8a), while it is expected that concrete porosity decreases with an increase in f_c and the corresponding decrease in the water–cement ratio. Second, while there is no clear correlation between δ_0 and concrete properties, there is a very strong linear correlation between δ_0 and t_{cr}. The most plausible explanation of these contradictions is that the assumption that corrosion products diffuse into the surrounding concrete only until they fully fill a finite-thickness "porous" zone is incorrect. Although a thin high-porosity zone exists at the concrete-reinforcing bar interface (its thickness may be between 2 and 8 μm as measured by Petre-Lazar [26]) corrosion products diffuse into the surrounding concrete constantly over time and not only until they fully fill this zone. This explains the strong linear correlation between δ_d and t_{cr} and is also supported by experimental observations, when corrosion products were detected in concrete pores several millimetres (or even centimetres) away from the corroded steel surface [12, 33].

It is also observed that the ratio of δ_d to $\delta_{cr,exp}$, i.e., the amount of corrosion products diffused into the surrounding concrete to the total amount of the corrosion products formed by the time of cover cracking, does not depend on t_{cr} (see Fig. 9). Based on this observation it is proposed to account for the diffusion of corrosion products into the surrounding concrete by assuming that this ratio, denoted further as η, is a time-independent constant. Since $(\delta_{cr} + \delta_d)$ in Eq. 33 represents the total amount of the corrosion products formed by the time of cover cracking and

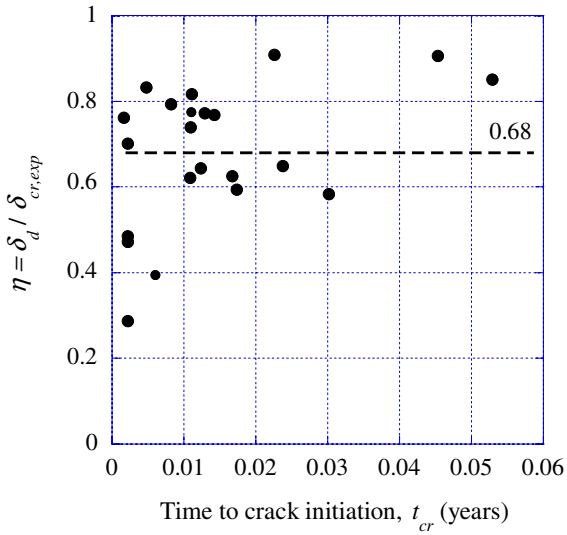

Fig. 9 The ratio η versus time to crack initiation

$\eta = \delta_d/(\delta_{cr} + \delta_d)$, it can easily be shown that $(\delta_{cr} + \delta_d)$ equals $\delta_{cr}/(1-\eta)$. Substituting the latter formula into Eq. 33 the following expression for evaluation of the time to crack initiation (in years) is obtained

$$t_{cr} = \frac{\delta_{cr}}{11.6 i_{corr}(\alpha_v - 1)(1-\eta)} \quad (37)$$

where i_{corr} is in μA/cm^2 and δ_{cr} in μm.

According to the results in Fig. 9, which have been obtained using data from accelerated corrosion tests with impressed current, the average value of η equals 0.68. Based on data from corrosion tests in natural conditions [5] a slightly higher average value of η of 0.73 has been found. Thus, it is tentatively recommended to set η equal to 0.70. Figure 10 shows comparison of the times to crack initiation predicted using the proposed model (i.e., Eq. 37), in which δ_{cr} is calculated in accordance to the procedure described in Sect. 3.4) to those observed in accelerated corrosion tests [3, 25, 28–32]. Values of the predicted times are given along the vertical axis while those observed in the tests—along the horizontal one; thus, in the case of perfect prediction the point should lie on the line bisecting the positive quarter of the coordinate system. As can be seen, a good agreement between the analytical and test results is observed. However, further experimental studies of corrosion-induced cover cracking, especially those involving natural corrosion, are needed.

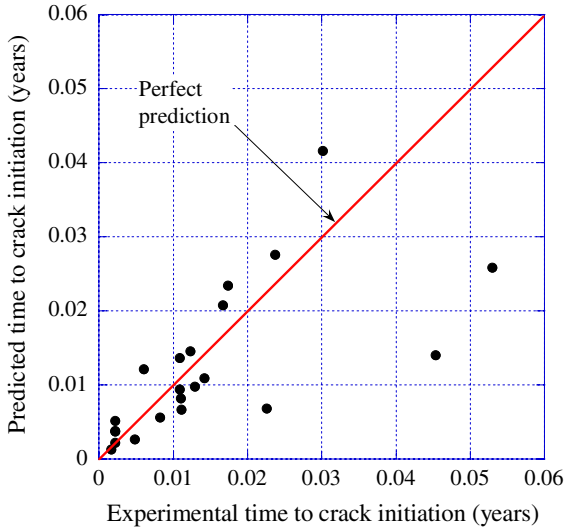

Fig. 10 Comparison of analytical and experimental results

5 Conclusions

In the paper a critical overview of existing analytical models for concrete cover cracking due to corrosion of reinforcing steel has been presented. Shortcomings and inconsistencies of the models have been discussed. A new theoretically sound and consistent analytical model have been presented. The model has been calibrated using available experimental data. The model has been used to estimate the amount of corrosion products diffused into the surrounding concrete. It has been shown that this amount may be higher than has been previously assumed and the assumption that corrosion products diffuse into the surrounding concrete only until they fully fill the "porous" zone leads to physically meaningless results. A new approach to account for the diffusion of corrosion products into the surrounding concrete has been proposed. Comparison of the times to crack initiation obtained using the proposed model with those observed in accelerated corrosion tests has been presented with a good agreement observed.

Acknowledgement This research was supported by the Bernstein Research Fund at the Technion.

References

1. Bentur A, Diamond S, Berke NS (1997) Steel corrosion in concrete. E&FN Spon, London
2. Val DV (2005) Effect of different limit states on life-cycle cost of RC structures in corrosive environment. J Infrastruct Syst 11(4):231–240. doi:10.1061/(ASCE)1076-0342(2005)11:4(231)
3. Alonso C, Andrade C, Rodriguez J, Diez JM (1998) Factors controlling cracking of concrete affected by reinforcement corrosion. Mater Struct 31:435–441. doi:10.1007/BF02480466
4. Bazant ZP (1979) Physical model for steel corrosion in concrete sea structures—application. J Struct Div 105(6):1155–1166
5. Liu Y, Weyers RE (1998) Modeling the time-to-corrosion cracking in chloride contaminated reinforced concrete structures. ACI Mater J 95(6):675–681
6. Li CQ, Melchers RE, Zheng JJ (2006) Analytical model for corrosion-induced crack width in reinforced concrete structures. ACI Struct J 103(4):479–487
7. Molina FJ, Alonso C, Andrade C (1993) Cover cracking as a function of rebar corrosion: part 2—numerical model. Mater Struct 26:532–548. doi:10.1007/BF02472864
8. Du YG, Chan AHC, Clark LA (2006) Finite element analysis of the effects of radial expansion of corroded

reinforcement. Compos Struct 84:917–929. doi:10.1016/j.compstruc.2006.02.012
9. Lekhnitskii SG (1981) Theory of elasticity of an anisotropic body. Mir, Moscow
10. Williamson SJ, Clark LA (2000) Pressure required to cause cover cracking of concrete due to reinforcement corrosion. Mag Concr Res 52(6):455–467
11. Timoshenko SP, Goodier JN (1982) Theory of elasticity. McGraw-Hill, New York
12. Newhouse CD, Weyers RE (1996) Modeling the measured time to corrosion cracking. In: Techniques to assess the corrosion activity of steel reinforced concrete structures. ASTM STP 1276, American Society for Testing and Materials, pp 3–22
13. Chernin L, Val DV (2008) Prediction of cover cracking in reinforced concrete structures due to corrosion. In: Proceedings of the 1st international conference on construction heritage in coastal and marine environments (MEDACS08), LNEC, Lisbon, 28–30 January 2008 (CD-Rom)
14. El Maaddawy T, Soudki K (2007) A model for prediction of time from corrosion initiation to corrosion cracking. Cem Concr Compos 29:168–175. doi:10.1016/j.cemconcomp.2006.11.004
15. ABAQUS (2004) ABAQUS user's manual, version 6.5. Hibbit-Karlson-Sorensen Inc, Pawtucket
16. Val DV, Chernin L, Stewart MG (2009) Experimental and numerical investigation of corrosion-induced cover cracking in reinforced concrete structures. J Struct Eng 135(4):376–385
17. Tepfers R (1979) Cracking of concrete cover along anchored deformed reinforcing bars. Mag Concr Res 31(106):3–12
18. Wang XH, Liu XL (2004) Modelling effects of corrosion on cover cracking and bond in reinforced concrete. Mag Concr Res 56(4):191–199. doi:10.1680/macr.56.4.191.36306
19. CEB (1993) CEB-FIP Model Code 1990. Bulletin d'Information No. 213/214. Comité Euro-International du Béton, Lausanne
20. Nielsen CV, Bićanić N (2002) Radial fictitious cracking of thick-walled cylinder due to bar pull-out. Mag Concr Res 54(3):215–221. doi:10.1680/macr.54.3.215.38797
21. Bhargava K, Ghosh AK, Mori Y, Ramanujam S (2006) Model for cover cracking due to rebar corrosion in RC structures. Eng Struct 28:1093–1109. doi:10.1016/j.engstruct.2005.11.014
22. Pantazopoulou SJ, Papoulia KD (2001) Modeling cover-cracking due to reinforcement corrosion in RC structures. J Eng Mech 127(4):342–351. doi:10.1061/(ASCE)0733-9399(2001)127:4(342)
23. George EA, Richard A, Ranjan R (1999) Special functions. Cambridge University Press, Cambridge
24. Suda K, Misra S, Motohashi K (1993) Corrosion products of reinforcing bars embedded in concrete. Corros Sci 35:1543–1549. doi:10.1016/0010-938X(93)90382-Q
25. Vu K, Stewart MG, Mullard J (2005) Corrosion-induced cracking: experimental data and predictive models. ACI Struct J 102(5):719–726
26. Petre-Lazar I (2000) Aging assessment of concrete structures submitted to steel corrosion (in French). PhD Thesis, Laval University, Quebec, Canada
27. CSA A23.3-94 (1994) Design of concrete structures. Canadian Standards Association, Rexadle, ON, Canada
28. Cabrera JG, Ghoddoussi P (1992) The effect of reinforcement corrosion on the strength of the steel/concrete bond. In: Proceedings of the international conference on bond in concrete, CEB, Riga, Latvia, 11–24 October
29. Andrade C, Alonso C, Molina FJ (1993) Cover cracking as a function of bar corrosion: part 1—experimental test. Mater Struct 26:453–464. doi:10.1007/BF02472805
30. Mangat PS, Elgarf MS (1999) Bond characteristics of corroding reinforcement in concrete beams. Mater Struct 32:89–97. doi:10.1007/BF02479434
31. El Maaddawy T, Soudki K, Topper T (2005) Long-term performance of corrosion-damaged reinforced concrete beams. ACI Struct J 102(5):649–656
32. Al-Harthy AS, Mullard J, Stewart MG (2007) Cracking in concrete due to corrosion of steel reinforcement. In: Proceedings of the 5th international conference on concrete under severe conditions: environment & loading (CONSEC'07), Tours, France (CD-Rom)
33. Marcotte TD, Hansson CM (2007) Corrosion products that form on steel within cement paste. Mater Struct 40:325–340. doi:10.1617/s11527-006-9170-4